第 31 卷第 9 期
2015 年 9 月

无 机 化 学 学 报
CHINESE JOURNAL OF INORGANIC CHEMISTRY

Vol.31 No.9
1785-1779

# 颜色可区分的氰桥五边形带经亲铜作用聚集的异金属多形体

秦英恋[1,2] 李士利[1] 姜 宁[1] 张献明*,[1]

([1]山西师范大学化学与材料科学学院,分子磁体与磁信息材料重点实验室,临汾 041004)

([2]运城学院应用化学系,运城 044000)

**摘要**: 水热条件下,环境友好的 $K_2[Ni(CN)_4]$能缓慢水解形成 *cis*-$[Ni(CN)_2(H_2O)_4]$单元和氰基配体,并进一步与金属铜(I)原子组装形成异金属的五边形带。这些五边形带通过亲铜聚集作用形成二维有色的超分子多形体$[(CuCN)_2Ni(CN)_2(H_2O)_4]$ (**1** 和 **2**)。研究发现,低温条件下形成了密集态的深蓝色的化合物 **1**,然而高温反应条件形成疏松态的紫色化合物 **2**,这一现象与高温高压的反应条件形成密集态的物质这一规律相违背。结构的进一步分析发现五边形环尺寸的微小改变和二维超分子层间距离的差异是引起这一反常的原因。除此之外,这两个新的化合物也是少见的由亲铜性聚集作用诱导的着色异常的多形体的例子,显示了从深蓝色到紫色的颜色改变。磁性研究证实了平面正方形的$[Ni(CN)_4]^{2-}$中的金属镍(Ⅱ)转换成了有着基态自旋 $S$=1 的八面体配位几何中心。

**关键词**: 亲铜作用; 多形体; 异金属; 五边形; 聚集

**中图分类号**: O614.121 **文献标识码**: A **文章编号**: 1001-4861(2015)09-1785-13

**DOI**:10.11862/CJIC.2015.249

# Distinguishable Polymorphs in Color: Cyano-Bridged Heterometallic Pentagonal Ribbons via Cuprophilic Aggregation

QIN Ying-Lian[1,2] LI Shi-Li[1] JIANG Ning[1] ZHANG Xian-Ming*,[1]

([1]*School of Chemistry & Material Science, Key Laboratory of Magnetic Molecules and Magnetic Information Material, Ministry of Education, Shanxi Normal University, Linfen, Shanxi* 041004, *China*)

([2]*Department of Applied Chemistry, Yuncheng University, Yuncheng, Shanxi* 044000, *China*)

**Abstract**: By using environmentally friendly $K_2[Ni(CN)_4]$ that slowly hydrolyse upon hydrothermal treatment, cis-$[Ni(CN)_2(H_2O)_4]$ units and cyanides were generated and further assembled with Cu(I) atoms into pentagonal heterometallic ribbons. Subsequently, these pentagonal ribbons are induced aggregation via cuprophilic interactions into 2D supramolecular coloured polymorphs $[(CuCN)_2Ni(CN)_2(H_2O)_4]$ (**1** and **2**). Dark blue **1** synthesized at a lower temperature is a denser phase while purple **2** synthesized at a higher temperature is a looser phase, which is abnormal to general rule that a higher reaction time and pressure tends to form a denser phase. Careful examination on structures reveals that slight size difference in pentagons and different interlayer distances of 2D supramolecular arrangement contribute to the abnormality. Besides, the titled compounds could be rare cuprophilicity drived examples of coloured polymorphs, which exhibit remarkable colour difference from dark-blue to purple. Magnetic measurements confirmed that diamagnetic Ni(Ⅱ) atom in square planar $[Ni(CN)_4]^{2-}$ is transformed into octahedral coordinated Ni(Ⅱ)with ground state spin $S$=1. CCDC: 1046750, **1**; 1046751, **2**.

**Key words**: cuprophilicity; polymorph; heterometa; pentagon; aggregate

收稿日期:2015-04-20。收修改稿日期:2015-06-05。

国家重点基础研究发展计划(973 项目 2012CB821701),中国教育部项目(No.IRT1156), 国家杰出青年科学基金(No.20925101),运城学院青年教师科研启动项目(No.YQ-2013013)资助。

*通讯联系人。E-mail:zhangxm@dns.sxnu.edu.cn

## 0 Introduction

The attractive interactions between closed-shell $d^{10}$ metal ions have received considerable attention because they play an important role in the structural, optical, and electronic properties that are associated with the presence of metallophilicity effect[1]. This behavior has been frequently observed in Au, with the term "aurophilicity" being used to describe Au $^{I}$-Au $^{I}$ interactions that are theoretically attributed to correlation and relativistic effects[2-5]. The occurrence of analogous metallophilic effects has been found even in lighter Cu atoms, while most structurally characterized complexes featuring Cu $^{I}$-Cu $^{I}$ interactions, namely, "cuprophilicity", are associated with the other structure-controlling factors, such as ligand bridging, H bonding, electrostatic interaction, $\pi$-$\pi$ stacking, *etc*[6-8]. It is well recognized that only a few reliable cases of cuprophilicity have been reported and the phenomenon of cuprophilicity is usually encountered in a classic family of oligomers, dimers, trimers and chains complexes[9-11]. Theoretical studies reveal that the strength of cuprophilicity is up to 17 kJ·mol$^{-1}$, indicating cuprophilicity may be used as synthons for control over supramolecular polymorphs[12]. Recently, we and others have endeavored to modulate multidimensional CuCN-based supramolecular frameworks via cuprophilic interactions[13-14]. In some rare cases, CuCN-based supramolecular isomers with cuprophilic interactions have been prepared.

On the other hand, chromism is a process that induces a change in the colors of compounds. In most cases, chromism is based on a change in the electron states of molecules, so this phenomenon induced by various external stimuli *e.g.*, solvents, applied stress, pH value, temperature, *etc*[15-16]. Differing from the above external stimulation, supramolecular cuprophilicity can induce aggregation of various of coordination geometry of copper(I) to give broad range of colors crystal forms in the solid state and show interesting absorption and luminescence effect related to electron modulation by cuprophilic interactions[9-11]. The sensitivity of the electronic absorption and luminescence properties to the degree of cuprophilic interactions may offer an attractive option for the exploitation of color change of different crystal forms in the solid state[17-18]. To date, although the cuprophilicity-induced CuCN-based monometallic polymorphic phenomena are well known, most systems are confined to studies of their structures and crystal packings in the solid state, with corresponding studies on crystal color-varied phenomena arising from cuprophilic aggregation less explored[13-14]. As an extension of our work on cuprophilicity controlled complexes, we report two heterometallic cyano-bridged color-varied isomorphisms [$(CuCN)_2Ni(CN)_2(H_2O)_4$] (**1** and **2**), both of which have two dimensional supramolecular arrays constructed pentagonal heterometallic ribbons via different extent of Cu $^{I}\cdots$ Cu $^{I}$ interactions. Quite interestingly, dark blue isomorphism **1** synthesized a lower temperature and pressure has weaker Cu $^{I}\cdots$ Cu $^{I}$ interaction but larger density while purple isomorphism **2** synthesized a higher temperature and pressure has stronger Cu $^{I}\cdots$ Cu $^{I}$ interactions but smaller density. This kind of abnormality between pressure and density can be rationalized by analyses of the size of pentagonal rings and distances between adjacent 2D layers.

## 1 Experimental

### 1.1 Materials and methods

All chemicals were analytically pure from commercial sources and used without further purification. Elemental analyses were performed on a Vario EL-Ⅱ analyzer. FTIR spectra were recorded from KBr pellets in the range 4 000~400 cm$^{-1}$ on a Perkin-Elmer Spectrum BX FTIR spectrometer. Powder X-ray diffraction (PXRD) data were collected in a Bruker D8 advance diffractometer. The magnetic measurements were made with Quantum Design SQUID MPMS XL-5 instruments. The diamagnetic correction for each sample was applied using Pascals constants. Scanning electron microscope Energy-disperse X-ray spectroscopy analysis (SEM-EDS) were measured on a JSM-7500F equipped with an EDAX CDU leap detector. The thermogravimetric analysis (TG/DTA) were carried out in air atmosphere using SETARAM

LABSYS equipment at a heating rate of 10 ℃·min$^{-1}$. The UV-Vis diffuse reflection curves were performed on the powder samples in the room temperature through TU-1901 double beam spectrophotometer.

### 1.2 Syntheses of compounds 1 and 2

#### 1.2.1 Synthesis of compound **1**

A mixture of $CuCl_2 \cdot 2H_2O$ (0.068 g, 0.4 mmol), $K_2[Ni(CN)_4]$ (0.084 g, 0.2 mmol), aqueous ammonia (25%, 2 mL) in a molar ratio of 2.0:1.0:14.8 and $CH_3CN$ (3 mL), and water (3 mL) was sealed in a 15 mL Teflon-lined stainless container, which was heated to 140 ℃ and held for 5 days. After cooling to room temperature, dark-blue block-like crystals of **1** were obtained with a yield of 45%. Elemental analysis Calcd. for **1** (%): C, 13.27; H, 2.22; N, 15.48; Found (%): C,13.34; H, 2.20, N, 15.58. IR (KBr, cm$^{-1}$): 2 104 (s), 1 608 (s), 1 247 (s), 1 180 (m), 678 (m), 3393 (w), 3278 (w).

#### 1.2.2 Synthesis of compound **2**

The preparation condition of **2** was same to **1** except that the temperature was increased to 145 ℃. After cooling to room temperature, purple block crystals of isomorphism **2** were recovered in 50% yield. Elemental analysis Calcd. for **2** (%): C, 13.27; H, 2.22; N, 15.48; Found (%): C, 13.24; H, 2.18, N, 15.45. IR (KBr, cm$^{-1}$): 2 107 (s), 1 612 (s), 1 245 (s), 1 180 (m), 681 (m), 3 390 (w), 3 284 (w).

### 1.3 X-ray data collection and structure determination

Data were collected at 298 K on a Bruker Apex diffractometer (Mo $K\alpha$, $\lambda$ =0.071 073 nm). Lorentz-polarization and absorption corrections were applied. The structures were solved with direct methods and refined with full-matrix least-squares technique (SHELX-97)[19]. Analytical expressions of neutral-atom scattering factors were employed, and anomalous dispersion corrections were incorporated. All non-hydrogen atoms were refined anisotropically. Hydrogen atoms of organic ligands were geometrically placed and refined with isotropic temperature factors. The crystallographic data and selected bond lengths and bond angles are listed in Table 1 and Table 2.

CCDC: 1046750, **1**; 1046751, **2**.

**Table 1　Crystallographic data for compounds 1 and 2**

| Compounds | **1** | **2** |
|---|---|---|
| Formula | $C_4H_8Cu_2N_4NiO_4$ | $C_4H_8Cu_2N_4NiO_4$ |
| Formula weight | 361.93 | 361.93 |
| Crystal system | Orthorhombic | Orthorhombic |
| Space group | *Cmca* | *Cmca* |
| $a$ / nm | 1.226 72(13) | 1.226 04(5) |
| $b$ / nm | 1.408 94(15) | 1.471 28(5) |
| $c$ / nm | 1.271 85(13) | 1.269 82(5) |
| $V$ / nm$^3$ | 2.198 23(15) | 2.290 56(15) |
| $Z$ | 8 | 8 |
| $D_c$ / (g·cm$^{-3}$) | 2.187 | 2.099 |
| $\mu$ / mm$^{-1}$ | 5.528 | 5.305 |
| $\theta$ range / (°) | 2.72~26.37 | 2.69~26.37 |
| $F$(000) | 1 424 | 1 424 |
| Size / mm | 0.42×0.10×0.06 | 0.10×0.07×0.05 |
| Reflections collected / Unique | 5 516/1 179 | 8 343/1 228 |
| Reflections observed ($I>2\sigma$(I)) | 1 039 | 1 120 |
| $R_{int}$ | 0.031 8 | 0.024 5 |
| GOF on $F^2$ | 1.160 | 1.093 |
| $R_1$, $wR_2$ ($I>2\sigma$(I)) | 0.056 0, 0.169 2 | 0.036 7, 0.102 8 |
| $R_1$, $wR_2$ (all data) | 0.063 5, 0.185 2 | 0.040 0, 0.105 3 |
| $(\Delta\rho)_{max}$, $(\Delta\rho)_{min}$ / (e·nm$^{-3}$) | 1 322 , −775 | 921 , −769 |

**Table 2 Selected bond lengths (nm) and angles (°) for compounds 1 and 2**

| | | | | | |
|---|---|---|---|---|---|
| Compound **1** | | | | | |
| Cu(1)-N(1) | 0.192 9(7) | Ni(1)-O(2W) | 0.201 1(11) | Cu(1)-C(3) | 0.195 4(6) |
| Ni(1)-O(2Wb) | 0.201 1(11) | Cu(1)-C(2) | 0.198 3(6) | C(1)-N(1) | 0.113 4(10) |
| Cu(1)-Cu(1a) | 0.283 5(2) | C(2)-N(2c) | 0.109 5(12) | Ni(1)-C(1) | 0.203 8(6) |
| C(2)-C(2c) | 0.109 5(12) | Ni(1)-C(1b) | 0.203 8(6) | C(3)-N(3d) | 0.114 1(13) |
| Ni(1)-O(1W) | 0.207 1(13) | C(3)-C(3d) | 0.114 1(13) | Ni(1)-O(3W) | 0.215 0(10) |
| N(1)-Cu(1)-C(3) | 124.1(3) | C(1b)-Ni(1)-O(1W) | 91.2(3) | N(1)-Cu(1)-C(2) | 120.6(3) |
| O(2Wb)-Ni(1)-O(3W) | 90.2(5) | C(3)-Cu(1)-C(2) | 110.4(3) | O(2W)-Ni(1)-O(3W) | 90.2(5) |
| N(1)-Cu(1)-Cu(1a) | 65.3(2) | C(1)-Ni(1)-O(3W) | 92.9(3) | C(3)-Cu(1)-Cu(1a) | 114.0(2) |
| C(1b)-Ni(1)-O(3W) | 92.9(3) | C(2)-Cu(1)-Cu(1a) | 113.6(2) | O(1W)-Ni(1)-O(3W) | 173.7(5) |
| O(2Wb)-Ni(1)-O(2W) | 80.9(9) | N(1)-C(1)-Ni(1) | 172.3(7) | O(2Wb)-Ni(1)-C(1) | 90.8(5) |
| N(2c)-C(2)-C(2c) | 0.0(7) | O(2W)-Ni(1)-C(1) | 171.1(5) | N(2c)-C(2)-Cu(1) | 177.8(9) |
| O(2Wb)-Ni(1)-C(1b) | 171.1(5) | C(2c)-C(2)-Cu(1) | 177.8(9) | O(2W)-Ni(1)-C(1b) | 90.8(5) |
| N(3d)-C(3)-C(3d) | 0.0(7) | C(1)-Ni(1)-C(1b) | 97.4(4) | N(3d)-C(3)-Cu(1) | 170.9(2) |
| O(2Wb)-Ni(1)-O(1W) | 84.9(5) | C(3d)-C(3)-Cu(1) | 170.9(2) | O(2W)-Ni(1)-O(1W) | 84.9(5) |
| C(1)-N(1)-Cu(1) | 171.6(7) | C(1)-Ni(1)-O(1W) | 91.2(3) | | |
| Compound **2** | | | | | |
| Cu(1)-N(1) | 0.194 9(5) | Ni(1)-O(2W) | 0.213 4(4) | Cu(1)-C(2) | 0.196 6(4) |
| Ni(1)-O(2Wb) | 0.213 4(4) | Cu(1)-C(3) | 0.197 4(4) | C(1)-N(1) | 0.113 2(6) |
| Cu(1)-Cu(1a) | 0.273 81(11) | C(2)-N(2c) | 0.114 6(8) | Ni(1)-C(1) | 0.208 9(3) |
| C(2)-C(2c) | 0.114 6(8) | Ni(1)-C(1b) | 0.208 9(3) | C(3)-N(3d) | 0.114 4(8) |
| Ni(1)-O(3W) | 0.212 6(5) | C(3)-C(3d) | 0.114 4(8) | Ni(1)-O(1W) | 0.212 8(5) |
| N(1)-Cu(1)-C(2) | 119.32(17) | O(1W)-Ni(1)-O(2W) | 89.98(16) | N(1)-Cu(1)-C(3) | 124.26(17) |
| C(1)-Ni(1)-O(2Wb) | 90.30(15) | C(2)-Cu(1)-C(3) | 109.54(17) | C(1b)-Ni(1)-O(2Wb) | 177.33(15) |
| N(1)-Cu(1)-Cu(1a) | 64.61(14) | O(3W)-Ni(1)-O(2Wb) | 90.85(16) | C(2)-Cu(1)-Cu(1a) | 114.97(12) |
| O(1W)-Ni(1)-O(2Wb) | 89.98(16) | C(3)-Cu(1)-Cu(1a) | 116.97(12) | O(2W)-Ni(1)-O(2Wb) | 87.7(2) |
| C(1)-Ni(1)-C(1b) | 91.6(2) | N(1)-C(1)-Ni(1) | 172.4(4) | C(1)-Ni(1)-O(3W) | 90.97(15) |
| N(2c)-C(2)-C(2c) | 0.00(7) | C(1b)-Ni(1)-O(3W) | 90.97(15) | N(2c)-C(2)-Cu(1) | 177.5(5) |
| C(1)-Ni(1)-O(1W) | 88.23(15) | C(2c)-C(2)-Cu(1) | 177.5(5) | C(1b)-Ni(1)-O(1W) | 88.23(15) |
| N(3d)-C(3)-C(3d) | 0.0(4) | O(3W)-Ni(1)-O(1W) | 178.8(2) | N(3d)-C(3)-Cu(1) | 168.87(12) |
| C(1)-Ni(1)-O(2W) | 177.33(15) | C(3d)-C(3)-Cu(1) | 168.87(12) | C(1b)-Ni(1)-O(2W) | 90.30(15) |
| C(1)-N(1)-Cu(1) | 170.3(4) | O(3W)-Ni(1)-O(2W) | 90.85(16) | | |

Symmetry codes: a: $-x+1/2, -y+3/2, -z+1$; b: $-x+1, y, z$; c:$-x+1/2, y, -z+1/2$; d: $-x, y, z$

## 2 Results and discussion

### 2.1 Description of crystal structures

2.1.1 Crystal structure of compound **1**

Single-crystal X-ray analysis shows that dark-blue **1** and purple **2** are isostructural, and thus only the structure of **1** is described herein in detail. Dark-blue and denser **1** crystallizes in the orthorhombic space group *Cmca*, which has a larger calculated density of 2.187 $g \cdot cm^{-3}$. The asymmetric unit consists of one crystallographically independent Cu(Ⅰ) centers, half Ni(Ⅱ) atom, two cyanides and two water molecules as shown in Fig.1a. All atoms except for Cu (1), C(1), N (1) and O (2W) localize in general positions. The indistinguishable C (2), N (2), C (3) and N (3) atoms occupy same sites and have a site occupancy of 0.5.

The Ni(1), O(1W) and O(3W) atoms are within crystallographic mirror and thus have site occupancy of 0.5. The C(1)-N(1) distance of 0.1134(10) nm is the typical C ≡N bond length of cyanide. The Cu (1) adopts a trigonal geometry, coordinated by N(1), C(2)/N(2) and C(3)/N(3) from three different cyanides. The Cu (1)-N (N=cyanide) bond lengths are in the range of 0.192 9(7)~0.198 3(6) nm. The N-Cu(1)-N (N= cyanide) bond angles are in the range of 110.4 (3)°~124.1(3)°, which is close to 120° that can be viewed as close to trigonal-planar structure. The Ni(1) atom shows an octahedral coordination environment, being occupied by two *cis*-carbon atoms from cyanides and four terminal water molecules. The Ni(1)-C(1) bond length is equal 0.203 8(6) nm while the Ni(1)-O(W) bond distances are in the range of 0.201 1(11)~0.215 0(10) nm. The *cis*- and *trans*-L-Ni(1)-L (L=C, O) angles are in the range of 80.9(9)°~97.4(4)° and 171.1(5)°~173.7(5)°, suggesting a distorted octahedral geometry. The octahedral *cis*-$[Ni(CN)_2(H_2O)_4]$ units can be considered as 2-connected bridging with an approximate angle of 97.4(4)°.

Each Cu center is connected to two adjacent Cu centers and one Ni center via linearly coordinated cyanides to generate pentagonal neutral ribbon $[(CuCN)_2Ni(CN)_2(H_2O)_4]$ (Fig.1b). The basic units in the ribbon are 15-membered $[Cu_4Ni(CN)_5]$ ring pointing in opposite directions, in which the five sides are 0.500 13, 0.060 8, 0.506 08, 0.508 80 and 0.508 80 nm as well as the internal angles are 97.4(4)°, 110.4(3)°, 110.4(3)°, 120.6(3)° and 120.6(3)°, showing some deviation from ideal 108° internal angles of regular pentagon. The pentagon in **1** is also different from pentagonal Cairo tiling which has internal angles of 90° and 120°. It should be noted that there exist weak unsupported $Cu^{I}\cdots Cu^{I}$ interactions between adjacent ribbons with distances of 0.283 5(2) nm, by which the pentagonal ribbons are extended into 2-D supramolecular array (Fig.1c). The adjacent layers are stacked in an ABAB fashion, and the average interlayer distance is 0.704 47 nm along the *b* axis in **1** (Fig.1d). The terminal water molecules of Ni (1) atoms protrude out on two sides of the pentagonal with shortest inter-ribbon O ··· O distance of 0.332 1 nm, indicating negligible O-H ··· O hydrogen bonds and genuine unsupported cuprophilicity. The structure and formula of **1** are reminiscent of cyanide-based mixed-valence copper complex $\{Cu^{II}(NH_3)_3Cu^{I}(CN)[Cu^{I}(CN)_3]\}_n$[20], in which cyanides bridge between $Cu^{II}$ and $Cu^{I}$ ions to form a centipede-like belt containing 15-memebered $[Cu^{I}_4Cu^{II}(CN)_5]$ pentagonal rings. In contrast, the compound **1** exhibits cyanide-based heterometallic pentagonal ribbons composed of heterometallic 15-membered basic units $[Cu^{I}_4Ni^{II}(CN)_5]$, in which octahedral coordinated *cis*-$[Ni^{II}(CN)_2(H_2O)_4]$ units formed by square planar $[Ni(CN)_4]^{2-}$ slowly hydrolyze upon hydrothermal treatment.

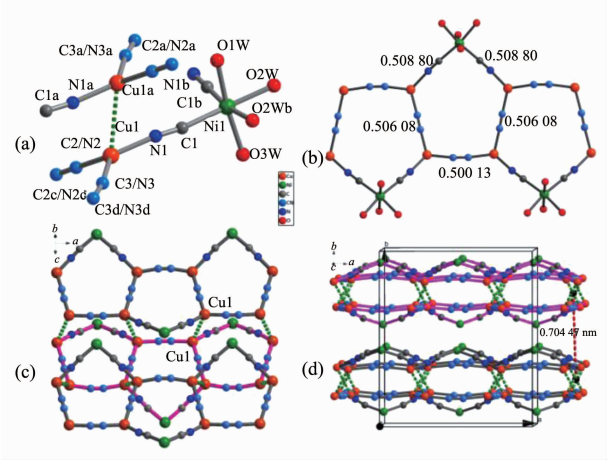


Fig.1　View of the coordination environments of metal atoms (a), 1-D pentagonal ribbon of 15-membered $[Cu_4Ni^{II}(CN)_5]$ rings (b), the 2-D supramolecular array showing unsupported $Cu^{I}\cdots Cu^{I}$ interactions (green dashed lines) (c) and the ABAB stacking of adjacent layers (d) along the *b* axis in compound **1**

2.1.2 Crystal structure of compound **2**

Keeping the same molar ratio and increasing the temperature to 145 ℃, purple **2** was obtained, which also crystallizes in the orthorhombic space group Cmca. Careful structure analysis has revealed that the two compounds are identical in chemical composition and coordination modes, as well as extended 2-D supramolecular arrays and packing modes of adjacent layers, but they possess different bond lengths and angles and strength of unsupported $Cu^{I}\cdots Cu^{I}$ interactions (0.283 5(2) nm in **1** and 0.273 81(11) nm in **2**) (Table 2). Notably, the significant changes in bond lengths and angles may result in a little expanded $[Cu_4Ni(CN)_5]$ pentagonal rings in **2**, which can be seen from five side distances (0.501 84, 0.515 91, 0.515 91, 0.507 75 and 0.507 75 nm) (Fig. 2a). Furthermore, slightly expanded pentagonal rings also respond to the average interlayer distance of 0.735 64 nm in **2** longer than 0.704 47 nm of **1** along the *b* axis (Fig.2b). Considering the above points, we conclude that the larger size of pentagonal rings and relatively longer distance of interlayer responsible for a looser structure and a smaller density of 2.099 $g\cdot cm^{-3}$ in **2** than 2.187 $g\cdot cm^{-3}$ of **1**, which is in accordance with the increased cell volume by 4.2% (Table 1). Similarly, the shortest inter-ribbon O⋯O distance is 0.362 5 nm for **2**, fully eliminating O-H⋯O hydrogen interaction and exhibiting genuine cuprophilicity.

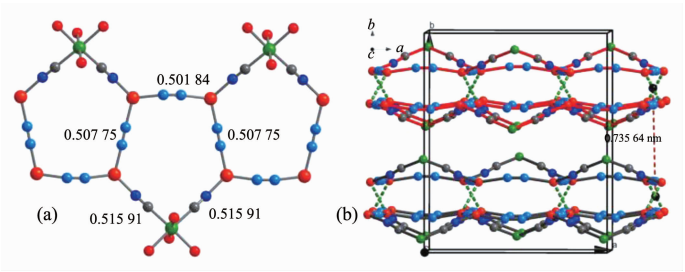


Fig.2 1-D pentagonal ribbon formed by larger size of 15-membered $[Cu_4Ni^{II}(CN)_5]$ pentagonal rings compared with **1** (a), the ABAB stacking of adjacent layers along the b axis showing longer distances of interlayer in **2** (b)

Although the theoretical and experimental studies of metallophilicity for the closed-shell $d^{10}$ metal ions have been widely documented, examples of ligand unsupported $Cu^{I}\cdots Cu^{I}$ interactions are relatively few, as compared to those of ligand unsupported $Au^{I}$-$Au^{I}$ and $Ag^{I}$-$Ag^{I}$ interactions[9-11]. The examples of complexes with ligand-unsupported cuprophilicity are very important for the study of this kind of optics and electricity related weak interactions. The cuprous cyanide system could give an opportunity to investigate metallophilic interactions because the ligand steric hindrance and inter-chain copper-ligand interactions are decreased in the system. It should be noted that the $Cu^{I}\cdots Cu^{I}$ distances of 0.283 5 nm in **1** and 0.273 8 nm in **2**, closer and slightly shorter than the sum of van der Waals radii for dicoordinated Cu(I) atoms (0.280 nm), are not associated with ligand-bridged, hydrogen bonded, electrostatic attracted and $\pi$-$\pi$ stacked effects, and thus they indicate reliable unsupported $Cu^{I}\cdots Cu^{I}$ interactions. To date, there are only a few ligand-unsupported cuprophilic interactions; these are usually constructed by linear two-coordinate Cu(I) centers, such as $[Cu(NH_3)Cl]$ (0.297 9(1) nm)[9a], $[Cu(NH_3)_2]Br$ (0.293 1(1) nm)[9a], $([CuCl_2]^-)_2$ (0.292 2(2) nm)[9b] and $[^tBuCu(CN)Li\cdot(OEt_2)_2]_8$ (0.271 3(1) nm)[9c]. To our knowledge, only few examples featuring trigonal Cu(I) centers have been reported in $[Cu_3\{2\text{-}[3(5)\text{-}pz]py\}_3]_2$ (0.290 5(3) nm)[9d] and $[Cu_2(obpy)_2]_2$ (0.298 6 and 0.299 3 nm)[6a]. Differently, cuprophilic interactions in **1** and **2** are formed between inter-ribbon three-coordinated copper centers and have shorter $Cu^{I}\cdots Cu^{I}$ distances. The preparation and structural characterization of **1** and **2** show that cuprophilicity as one kind of weak supramolecular force, can be used as synthons for control over supramolecular polymorphous compounds.

### 2.2 Relationship between synthesis and structure chemistry

Hydrothermal reactions of $CuCl_2$, $K_2[Ni(CN)_4]$ and aqueous ammonia in the same molar ratio synthesized denser dark-blue **1** (2.187 g·cm$^{-3}$) at a lower temperature of 140 ℃ and looser purple polymorph **2** (2.099 g·cm$^{-3}$) at a higher temperature of 145 ℃ (Scheme 1). As can be seen, 5 ℃ difference in reaction temperature is enough to affect strength of unsupported $Cu^{I}\cdots Cu^{I}$ interactions and overall supramolecular arrays. The $Cu^{I}\cdots Cu^{I}$ distances in **1** and **2** are ca. 0.283 5 and 0.273 8 nm, respectively, which means a stronger cuprophilicity in **2**. As confirmed by crystallographic study, the coordination geometries for metal ions, pentagonal ribbons and packing fashion of ribbons are very similar in **1** and **2**. Thus one may expect that **2** has a larger density due to shorter and stronger $Cu^{I}\cdots Cu^{I}$ contact. However, this is not the case. Compound **2** is lighter than 1 by 4.2% . What is the abnormal reason? Careful examinations reveal that the larger size of $[Cu_4Ni(CN)_5]$ pentagonal rings and relatively longer distances between 2D layers in **2** contribute to the abnormal phenomenon, which is in accordance with the deviation distance of *b* axis from 1.408 to 1.471 nm. Generally, polymorphs with close formation entropy are obtained in mixture. Interestingly, **1** and **2** can be easily synthesized and separated due to quite different colors. Besides, the bulk purity of polymorphs **1** and **2** was verified by contrast of recorded and simulated XRPD patterns (Fig.3). Their simulated XRPD patterns are very similar and the small differences are caused by the small different unit-cell parameters. The evidence of bridging cyanide groups is provided by the presence of cyanide group stretching absorptions at 2 107 cm$^{-1}$ for **1** and at 2 104 cm$^{-1}$ for **2** in the infrared spectra (Fig.4). The presence of heterometallic Ni(Ⅱ) atoms in **1** and **2** was confirmed by EDS analyses (Fig.5 and Table 3) and magnetic analysis.

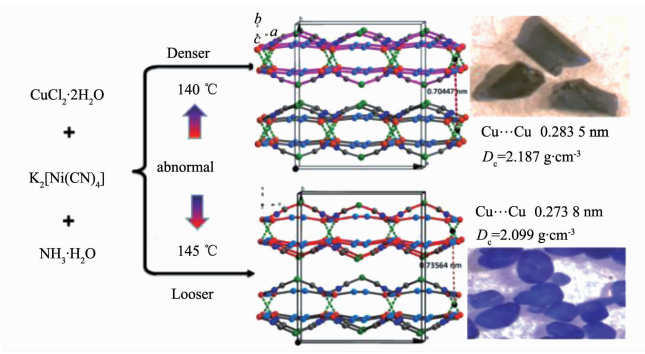


Scheme 1　View of syntheses and supramolecular packing, and photographs in polymorphs

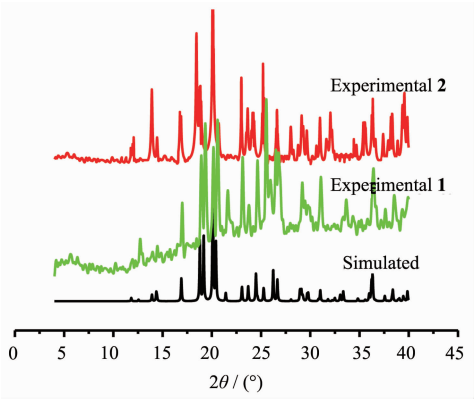


Fig.3　Simulated and measured XRPD patterns for **1** and **2**

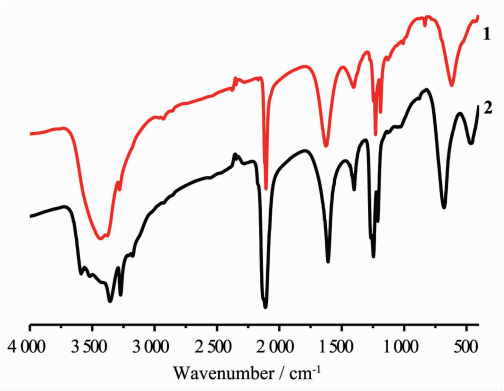


Fig.4 IR spectra of **1** and **2**

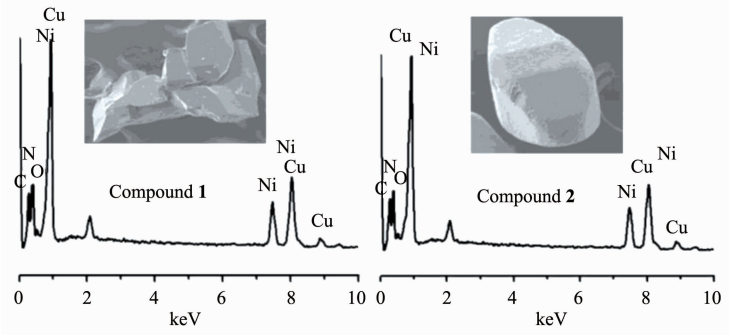


Fig.5 SEM images and EDS plots for **1** and **2**

**Table 3 Elemental analysis C, H and N and EDS data for ratio of Cu and Ni in heterometallic 1 and 2**

| Polymorphs | C, H, N analyses Found(Calcd.) / % | EDS results ($n_{Cu}$:$n_{Ni}$) | Single-crystal diffraction data ($n_{Cu}$:$n_{Ni}$) |
|---|---|---|---|
| **1** | 13.34, 2.20, 15.58 (13.27, 2.22, 15.48) | 1.92:1.0 | 2.0:1.0 |
| **2** | 13.24, 2.18, 15.45 (13.27, 2.22, 15.48) | 1.96:1.0 | 2.0:1.0 |

## 2.3 Possible mechanism

Compared with traditional cyanide sources of KCN and CuCN, environmentally friendly cyanidometallate $K_2[Ni(CN)_4]$ can slowly release cyanide and act as heterometallic source upon heat treatment, which is a key for the formation of heterometallic **1** and **2**. This course can be expressed by the following equation:

$$[Ni(CN)_4]^{2-} + 4H_2O = [Ni(CN)_2(H_2O)_4] + 2CN^- \quad (1)$$

$$[Ni(CN)_2(H_2O)_4] + 2CN^- + 2Cu^+ = [(CuCN)_2Ni(CN)_2(H_2O)_4] \quad (2)$$

$$\text{Total}: [Ni(CN)_4]^{2-} + 4H_2O + 2Cu^+ = [(CuCN)_2Ni(CN)_2(H_2O)_4] \quad (3)$$

From a thermodynamic point of view, the stability constant of square planar $[Ni(CN)_4]^{2-}$ is very large ($K$= $2.0\times10^{31}$), indicating high chemical stability[21]. In spite of high stability, there exists a hydrolysis equilibrium between $[Ni(CN)_4]^{2-}$ and *cis*-$[Ni(CN)_2(H_2O)_4]$ as shown in Equation **1**. This equilibrium seems to be critical in the syntheses of **1** and **2**, and it should be noted that this course is accompanied by transition of strong square planar field to weak octahedral field for Ni(Ⅱ) atoms. The in situ formed minor *cis*-$[Ni(CN)_2(H_2O)_4]$ and $CN^-$ ions in the presence of Cu(Ⅰ) atoms can generate polymeric pentagonal ribbons that are aggregated via unsupported cuprophilic interaction into solids of **1** and **2**. Crystallization under

**Table 4　Relative bonding energies (ΔE) of the optimized building block $K_2[Ni(CN)_4]$, $H_2O$, $[Ni(CN)_2(H_2O)_4]$ and HCN and all of the calculations were performed at the DFT level by using the Gaussian 03 program package**

| Relative Building Block | | $K_2[Ni(CN)_4]$ | $H_2O$ | $[Ni(CN)_2(H_2O)_4]$ | HCN |
|---|---|---|---|---|---|
| Bonding energies | $\Delta E$ / (kJ·mol$^{-1}$) | −1 792.62 | −329.99 | −2 210.16 | −459.58 |
| | $\Delta E$ / eV | −77.735 1 | −14.309 7 | −95.841 7 | −19.929 2 |

Inset: Absorption spectra in visible region

hydrothermal condition can be a nonequilibrium course, which is helpful to hydrolysis of $[Ni(CN)_4]^{2-}$ into *cis*-$[Ni(CN)_2(H_2O)_4]$. It is noteworthy that both chloride and cyanide can act as reducing agent to reduce Cu(Ⅱ) into Cu(Ⅰ). TD-DFT calculations were performed using the B3LYP method[22] and the 6-31G (d, p) basis set[23], which have also been used to theoretically predict the Equation **1** reaction and function as an assistant method to qualitatively analyse the formation of the **1** and **2**. The modified neutral model building blocks of $K_2[Ni(CN)_4]$, $H_2O$, $[Ni(CN)_2(H_2O)_4]$, and HCN adapted from the X-ray data have been used as structure component unit for calculations by using the Gaussian 03 program package[24]. Relative bonding energies analysis for block unit $K_2[Ni(CN)_4]$, $H_2O$, $[Ni(CN)_2(H_2O)_4]$ and HCN are −1792.62, −329.99, −2210.16 and −459.58 kJ·mol$^{-1}$. It is interesting to find that the energy difference between the product and reactants is about −16.74 kJ·mol$^{-1}$, which is consistent with our deductions that the reaction product should possess more stable energies than reactants (Table 4).

## 2.4　Colored polymorphs

Although isostructural **1** and **2** have same building units and similar pentagonal ribbons and 2D supramolecular arrays, surprisingly, they show significantly different color: dark-blue **1** and purple **2**. The solid state diffuse-reflectance UV-Vis spectra using $BaSO_4$ powder as a 100% reflectance reference were recorded to reveal this phenomenon. The absorption data was calculated from the reflectance. As shown in Fig.6, the absorption spectra of **1** and **2** have a very similar high energy UV absorption peaks at about 272 nm and 274 nm, which are assigned to cyano centered $\pi$-$\pi^*$ charge transfer (LC) processes. The bands in visible region are important and

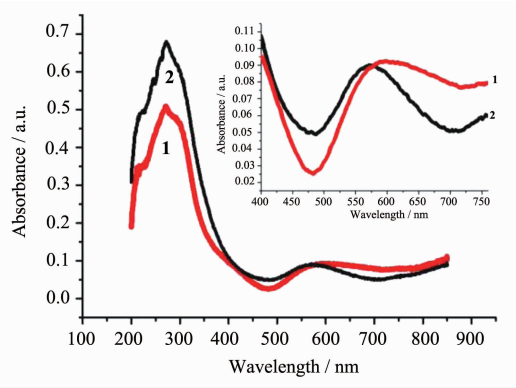


Fig.6　Solid-state UV-Vis absorption spectra of **1** and **2** at room temperature

responsible for the significant color difference. There is an absorption, which is started from 480 nm and extended to IR region with maxima at 590 nm for **1**. For **2**, there is also a visible absorption started from 480 nm and extended to IR region but the maximum absorption is *ca.* 570 nm, which is blue-shifted by 20 nm and has larger absorption intensity compared with **1**. This may explain the color difference of **1** and **2**. The visible absorption band at 590 nm and 570 nm that imparted the dramatic color difference has been tentatively assigned as a metal → metal $3d \rightarrow (4p, 4s)$ transition modified by cuprophilic interactions[17]. The UV-Vis spectra are in agreement with the color

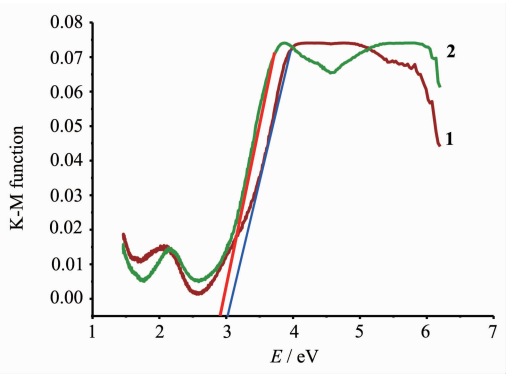


Fig.7　UV-Vis diffuse-reflectance spectra of K-M function vs energy of **1** and **2**

difference observed by naked eyes in our experiment. The band gaps of 3.00 eV and 2.92 eV for **1** and **2** have been measured by diffuse reflectivity for the powder sample, which indicate that they are potential semiconductor materials (Fig.7).

### 2.5 Thermogravimetry analysis

TG/DTA analyses for **1** and **2** in an air atmosphere and under 101 kPa pressure at the heating rate of 10 ℃·min$^{-1}$ were performed on polycrystalline samples, which showed similar thermal stability of **1** and **2**. This may be attributed to their similar supramolecular structures. As shown in Fig.8, TGA traces of **1** and **2** exhibit two main steps of weight loss. The initial weight loss of 17.71% for **1** and 18.1% for **2** occur in the temperature range of 129~280 ℃ and 122~297 ℃, which correspond to the loss of four water molecules (Calcd. 19.91%). The second weight loss of 29.5% for **1** and 27.4% for **2** occur in the temperature range of 349~1 080 ℃ and 361~1 085 ℃, which correspond to the removal of cyanides, and an intermediate of copper and nickel are formed by deduction from empirical composition (Calcd. 31.4%). DTA traces of **1** and **2** exhibit similar exothermic peak at ca. 425 ℃.

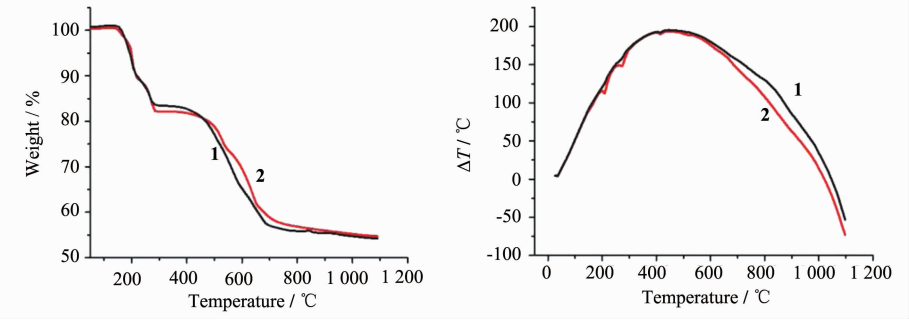


Fig.8 TGA-DTA curves of **1** and **2** in air atmosphere and at the heating rate of 10 ℃·min$^{-1}$

### 2.6 Magnetism

The temperature dependence of the magnetic susceptibilities for **1** and **2** in the temperature range of 2~300 K under 1 000 Oe applied field were measured with a Quantum Design SQUID MPMS XL-5. The $\chi_m T$ value at 300 K is 1.25 cm$^3$·K·mol$^{-1}$ for **1**, which is slightly larger than that expected 1.00 cm$^3$·K·mol$^{-1}$ for an uncoupled Ni(Ⅱ) ion with $g$=2.0. The $\chi_m T$ value decreases slowly with decreasing temperature until 50 K. After that, the $\chi_m T$ value rapidly decreases with lowering temperature down to a value of 0.34 cm$^3$·K·mol$^{-1}$ for **1** at 1.29 K. The tting of Curie-Weiss law in the temperature range of 20~300 K gives $C$=1.272 cm$^3$·K·mol$^{-1}$, $\theta$=–6.11 K (Fig.9a). The negative $\theta$ values indicate antiferromagnetic coupling dominating these systems. The $\chi_m T$ value at 300 K is 1.10 cm$^3$·K·mol$^{-1}$ for **2**, which is also slightly larger than that expected 1.00 cm$^3$·K·mol$^{-1}$ for an uncoupled Ni(Ⅱ) ion with $g$=2.0. The $\chi_m T$ value monotonically decreases to a value of 0.29 cm$^3$·K·mol$^{-1}$ at 2 K upon cooling. The

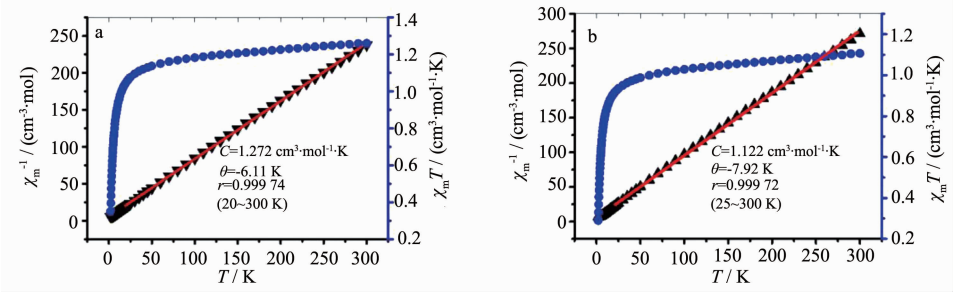


Red solid line represents the best fit

Fig.9 Magnetic susceptibility data per Ni1 unit presented as plots of $\chi_m T$ vs $T$ and $\chi_m^{-1}$ vs $T$ under an applied 1 000 Oe field for compounds **1** (a) and **2** (b)

tting of Curie-Weiss law in the temperature range of 25~300 K gives $C$=1.122 $cm^3 \cdot K \cdot mol^{-1}$, $\theta$=–7.92 K (Fig.9b). The field-dependent magnetization at 2 K increases slowly and linearly with the applied field, and no saturation is observed. The magnetization value at the highest field of 50 kOe are 1.52$N\beta$ for **1** and 1.46$N\beta$ for **2**, close to the saturation value of 2$N\beta$ expected for one spin-only Ni(Ⅱ) species (Fig.10). Quite a few examples of bimetallic systems containing diamagnetic cyanometalate bridging units between paramagnetic ions have been reported so far[25-26], in which weak antiferromagnetic exchange interactions are more likely due to a combination of intra- and inter-chain interactions.

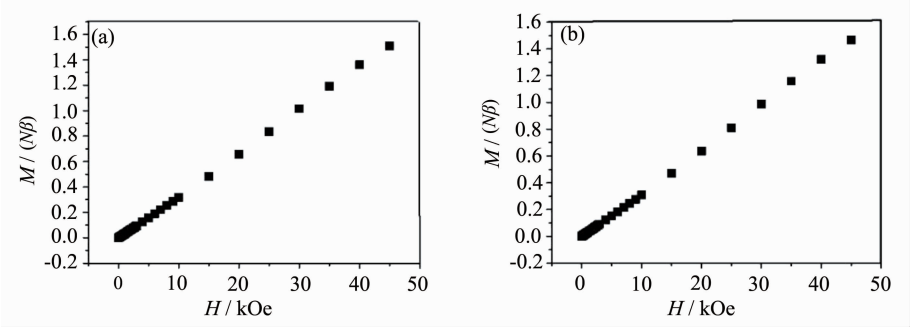


Fig.10　Field dependence of the magnetization per Ni1 unit at 2 K for **1** (a) and **2** (b)

## 3　Conclusions

In summary, we have demonstrated the preparation and characterization of two novel heterometallic polymorphs by using environmentally friendly $K_2[Ni(CN)_4]$ as cyanide source. Both consist of pentagonal heterometallic $[(CuCN)_2Ni(CN)_2(H_2O)_4]$ ribbons that are linked into 2D supramolecular arrays via unsupported cuprophilic interactions. Quite interestingly, dark blue **1** synthesized at a lower temperature and pressure is denser than purple **2** synthesized at a higher temperature and pressure. This observation is abnormal to general rule that a higher reaction temperature and pressure tends to form a dense phase, which can be rationalized by analyses of size of pentagonal rings and relative distances between adjacent layers. The size of $[Cu_4Ni(CN)_5]$ pentagons in **2** is a little larger than that in **1** and the distances between adjacent layers in **2** is also larger than that in **1**. Interesting color-varied phenomenon is observed in the two polymorphs, which is confirmed by remarkable color change from dark-blue to purple. UV-Vis absorption spectra are characteristic of two bands, in which the visible low energy one is responsible for different color and arising from $Cu^I \cdots Cu^I$ interactions. In situ slow hydrolysis of $[Ni(CN)_4]^{2-}$ to form *cis*-$[Ni(CN)_2(H_2O)_4]$ units and cyanides are key to formation of the two compounds, during which diamagnetic square planar Ni(Ⅱ) atom is transformed into octahedral coordinated Ni(Ⅱ) with ground state spin $S$=1. This work not only provide an environmentally friendly route to heterometallic cyanide polymorphs but also exhibit genuine cuprophilicity modulated optical behavior.

**References**:

[1] (a) Khlobystov A N, Blake A J, Champness N R, et al. *Coord. Chem. Rev.*, **2001**,**222**:155-192
(b) Yam V W W, Lo K K W. *Chem. Soc. Rev.*, **1999**,**28**:323-334
[2] (a) Zheng S L, Nygren C L, Messerschmidt M, et al. *Chem. Commun.*, **2006**,3711-3713
(b) Tong M L, Chen X M, Ye B H, et al. *Angew. Chem. Int. Ed.*, **1999**,**38**:2237-2239
(c) Ray L, Shaikh M M, Ghosh P. *Inorg. Chem.*, **2008**,**47**:230-240
[3] (a) Burini A, Fackler J P, Galassi R, et al. *J. Am. Chem. Soc.*, **2000**,**122**:11264-11265
(b) Streb C, Ritchie C, Long D L, et al. *Angew. Chem. Int. Ed.*, **2007**,**46**:7579-7582
[4] (a) Liu X, Guo G C, Fu M L, et al. *Inorg. Chem.*, **2006**,**45**:3679-3685
(b) Sun D F, Cao R, Weng J B, et al. *J. Chem. Soc. Dalton Trans.*, **2002**:291-292

[5] (a) Tong M L, Chen X M, Ye B H, et al. *Inorg. Chem*., **1998**,**37**:5278-5281
(b) Chen X M, Thomas C W M. *J. Chem. Soc. Dalton Trans*., **1991**:3253-3258
(c) Codina A, Fernández E J, Jones P G, et al. *J. Am. Chem. Soc*., **2002**,**124**:6781-6786

[6] (a) Zhang J P, Wang Y B, Chen X M, et al. *Chem. Eur. J*., **2005**,**11**:552-561
(b) Chui S S Y, Ng M F Y, Che C M, *Chem. Eur. J*., **2005**,**11**:1739-1749
(c) Sundararaman A, Zakharov L N, Jäkle F, et al. *Chem. Commun*., **2005**:1708-1710

[7] (a) Peng R, Li D, Wu T, et al. *Inorg. Chem*., **2006**,**45**:4035-4046
(b) Kang Y, Yao Y G, Qin Y Y, et al. *Chem. Commun*., **2004**:1046-1047

[8] (a) Cotton F A, Dikarev E V, Petrukhina M A, *Inorg. Chem*., **2000**,**39**:6072-6079
(b) Liu X, Guo G C, Liu B, et al. *Cryst. Growth Des*. **2005**, **5**:841-843
(c) Huang X C, Zhang J P, Chen X M, *J. Am. Chem. Soc*., **2004**,**126**:13218-13219

[9] (a) Margraf G, Bats J W, Bolte M, et al. *Chem. Commun*., **2003**:956-957
(b) Köhn R D, Seifert G, Pan Z, et al. *Angew. Chem. Int. Ed*., **2003**,**42**:793-796
(c) Boche G, Bosold F, Marsch M, et al. *Angew. Chem. Int. Ed*., **1998**,**37**:1684-1686
(d) Singh K, Long J R, Stavropoulos P. *J. Am. Chem. Soc*., **1997**,**119**:2942-2943

[10](a) Liu X, Guo G C, Wu A Q, et al. *Inorg. Chem*., **2005**,**44**:4282-4286
(b) Zhang X M, Tong M L, Gong M L, et al. *Chem. Eur. J*., **2002**,**8**:3187-3194
(c) Huang X C, Zhang J P, Chen X M. *Cryst. Growth Des*., **2006**,**6**:1194-1198
(d) Zheng S L, Messerschmidt M, Coppens P. *Angew. Chem. Int. Ed*., **2005**,**44**:4614-4617
(e) Zhang J X, He J, Yin Y G, et al. *Inorg. Chem*., **2008**,**47**:3471-3473

[11](a) Gao G F, Li M, Zhan S Z, et al. *Chem. Eur. J*., **2011**,**17**:4113-4117
(b) Jin K, Huang X, Pang L, et al. *Chem. Commun*., **2002**:2872-2873

[12]Hermann H L, Boche G, Schwerdtfeger P, *Chem. Eur. J*., **2001**,**7**:5333-5342

[13](a) Tronic T A, deKrafft K E, Pike R D, et al. *Inorg. Chem*., **2007**,**46**:8897-8912
(b) Lim M J, Murray C A, deButts J C, et al. *Inorg. Chem*., **2008**,**47**:6931-6947
(c) Hibble S J, Eversfield S G, Cowley A. R, et al. *Angew. Chem. Int. Ed*., **2004**,**43**:628-630
(d) Park K M, Lee S, Kang Y, et al. *Dalton Trans*., **2008**, 6521-6523

[14](a) Zhang X M, Hao Z M, Wu H S. *Inorg. Chem*., **2005**,**44**:7301-7303
(b) Qin Y L, Liu J, Zhang X M, et al. *Cryst. Growth Des*., **2012**,**12**:6068-6073
(c) Zhang X M, Qin Y L, Wu H S. *Inorg. Chem*., **2008**,**47**:2255-2257
(d) Qin Y L, Hou J J, Zhang X M, et al. *Cryst. Growth Des*., **2011**,**11**:3101-3108

[15](a) Reichardt C. *Chem. Rev*., **1994**,**94**:2319-2358
(b) Kahr B, Gurney R W. *Chem. Rev*., **2001**,**101**:893-952
(c) Sun J K, Cai L X, Zhang J, et al. *Chem. Commun*., **2011**, **47**:6870-6872
(d) Nakai H, Isobe K. *Coord. Chem. Rev*., **2010**,**254**:2652-2662

[16](a) Xu G, Guo G C, Huang J S, et al. *Angew. Chem. Int. Ed*., **2007**,**46**:3249-3251
(b) Létard J F, Guionneau P, Nguyen O, et al. *Chem. Eur. J*., **2005**,**11**:4582-4589
(c) Dias H V R, Diyabalanage H V K, Omary M A, et al. *J. Am. Chem. Soc*., **2003**,**125**:12072-12073

[17](a) Fu W F, Gan X, Che C M, et al. *Chem. Eur. J*., **2004**,**10**:2228-2236
(b) Che C M, Mao Z, Miskowski V M, et al. *Angew. Chem., Int. Ed*., **2000**,**39**:4084-4088
(c) Mao Z, Chao H Y, Che C M, et al. *Chem. Eur. J*., **2003**,**9**:2885-2894

[18](a) Che C M, Lai S W. *Coord. Chem. Rev*., **2005**,**249**:1296-1309
(b) He J, Yin Y G, Li D, et al. *Chem. Commun*., **2006**:2845-2847
(c) Yam V W W, Wong K M C, Zhu N. *J. Am. Chem. Soc*., **2002**,**124**:6506-6507
(d) Fu W F, Chan K C, Che C M, et al. *Chem. Eur. J*. **2001**,**7**:4656-4664
(e) Wong K M C, Yam V W W. *Acc. Chem. Res*., **2011**,**44**:424-434

[19]Sheldrick G M. *SHELX*-97, *Program for X-ray Crystal Structure Solution and Refinement*, Göttingen University, Germany, **1997**.

[20]Song Y, Xu Y, Wang T W, et al. *J. Mol. Struct*., **2006**,**788**:206-210

[21]ZHANG Xiang-Lin (张祥麟), KANG Heng (康衡). *Coordination Chemistry* (配位化学). Changsha: Zhongnan

Industrial University Press, **1986**.

[22](a) Becke A D. *J. Chem. Phys*., **1993**,**98**:5648

(b) Miehlich B, Savin A, Preuss H, et al. *Chem. Phys. Lett.*, **1989**,**157**:200

(c) Stephens P J, Devlin F J, Chabalowski C F. *J. Phys. Chem.*, **1994**,**98**:11623

[23]Petersson G A, Bennett A, Shirley W A, et al. *J. Chem. Phys.*, **1988**,**89**:2193

[24]Frisch M J, Trucks G W, Cheeseman J R. *Gaussian* 03, *Revision D*.01, Gaussian, Inc., Wallingford, CT, **2004**.

[25]Ohba M, Usuki N, Okawa H, et al. *Inorg. Chem*., **1998**,**37**: 3349-3354

[26]Rogez G, Marvilliers A, Mallah T, et al. *Angew. Chem. Int. Ed*., **2000**,**39**:2885-2887